ponentially decreasing concentration with fractional distance (Fig. 2B). The data define a linear decrease in concentration (*21*), for fractional distances greater than about 0.5, which is compatible with the episodic loss model for an event at 420 Ma (Fig. 2B).

A comparison of the data with diffusion models indicates that loss of ^{40}Ar in sample LA384A occurred by way of cylindrical volume diffusion, over a scale of 1000 μm, between about 460 and 420 Ma. Our preferred interpretation is that after retention of $^{40}Ar^*$ in the core of the crystal at 462 Ma, close to the timing of peak metamorphism, lower greenschist grade retrogression at 420 Ma formed the isotopic gradient. The sample did not experience substantial volume diffusion loss of $^{40}Ar^*$ after 420 Ma; however, $^{40}Ar^*$ was lost from areas inside the crystal that were deformed in Early Devonian time.

REFERENCES AND NOTES

1. M. A. Lanphere and A. L. Albee, *Am. J. Sci.* **274**, 545 (1974). We have recalculated all ages using the decay constants of R. H. Steiger and E. Jager [*Earth Planet. Sci. Lett.* **36**, 359 (1977)].
2. C. Chopin and H. Maluski, *Contrib. Mineral. Petrol.* **74**, 109 (1980).
3. J. R. Wijbrauns and I. McDougall, *ibid.* **93**, 187 (1989).
4. S. Scaillet, G. Feraud, Y. Lagabrielle, M. Ballevre, G. Ruffet, *Geology* **18**, 741 (1990).
5. S. Scalliet, G. Feraud, M. Ballevre, M. Amouric, *Geochim. Cosmochim. Acta* **56**, 2851 (1992).
6. K. de Jong, J. R. Wijbrans, G. Feraud, *Earth Planet. Sci. Lett.* **110**, 173 (1992).
7. D. Phillips and T. C. Onstott, *Geology* **16**, 542 (1988).
8. J. K. W. Lee, T. C. Onstott, J. A. Hanes, *Contrib. Mineral. Petrol.* **105**, 87 (1990).
9. S. P. Kelley and G. Turner, *Earth Planet. Sci. Lett.* **107**, 643 (1991).
10. Micas were hand-picked from the center of quartz lens LA384A after crushing and were irradiated in the core of the Los Alamos National Laboratory reactor (J = 0.01070 ± 0.00005). The neutron fluence was monitored with MMhb-1 [S. D. Sampson and E. C. Alexander, *Chem. Geol.* **66**, 27 (1987)], and reactions on K and Cl were also monitored with K_2SO_4 and KCl in the irradiation package. Crystals were cleaved into three sections on 001 with a scalpel, and a central section (200 μm thick) was analyzed with a MAP 215-50 mass spectrometer (sensitivity = 2.7×10^{-4} A/torr at an accelerating voltage of 3 kV, multiplier gain = 10,000). The signal evolution was linear during the analysis. Heating with a 10-W Coherent Ar-ion laser (0.25 to 1.0 s with a beam 25 μm in diameter) produced hemispherical melt pits 50 to 100 μm in diameter in the mica; melt pits were surrounded by a dehydration zone, and the overall diameter of the melting and dehydration region was roughly 150 μm. The size of the laser extraction pit was controlled to yield samples for which ^{40}Ar and ^{39}Ar were 50 to 300 times greater than the blank. An operational blank was analyzed after every five analyses in the present study, and nominal operational blanks were as follows: ^{40}Ar, 6×10^{-16} mol; ^{39}Ar, 1×10^{-17} mol; ^{38}Ar, 2×10^{-18} mol; ^{37}Ar, 1×10^{-17} mol; and ^{36}Ar, 5×10^{-18} mol. Radiogenic yields from the laser analyses were consistently greater than 85% and typically exceeded 95%. The precision of ^{40}Ar and ^{39}Ar measurements was generally about 0.5%, and the total error (combined J-value accuracy and sample precision) for ages was about ±1%.
11. J. Laird, M. A. Lanphere, A. L. Albee, *Am. J. Sci.* **284**, 376 (1984).
12. J. F. Sutter, N. M. Ratcliffe, S. B. Mukasa, *Geol. Soc. Am. Bull.* **96**, 123 (1985).
13. W. E. Hames, R. J. Tracy, N. M. Ratcliffe, J. F. Sutter, *Am. J. Sci.* **291**, 887 (1991).
14. F. M. Hueber, W. A. Bothner, N. L. Hatch, S. C. Finney, J. N. Aleinikoff, *ibid.* **290**, 360 (1990).
15. F. S. Spear and T. M. Harrison, *Geology* **17**, 181 (1989).
16. J. Crank, *The Mathematics of Diffusion* (Oxford Univ. Press, New York, ed. 2, 1975).
17. M. H. Dodson, *Contrib. Mineral. Petrol.* **40**, 259 (1973).
18. ———, *Mater. Sci. Forum* **7**, 145 (1986).
19. G. A. Robbins, thesis, Brown University (1972).
20. We substitute apparent age for concentration of $^{40}Ar^*$ in Eq. 1. Additional symbols for Eqs. 1 and 2 are as follows: t_a is apparent age, t_i is 462 Ma (the oldest ages from the core of the sample), t_e is the timing of the event of interest (either 420 or 390 Ma), a is the diffusion dimension, r is the radial distance, D is the diffusion coefficient, E is activation energy, t is the temperature of the loss event, α_n represents roots of the Bessel functions $J_0(x)$ and $J_1(x)$, R is the gas constant, and $G(x)$ and T are functions with tabulated values (*18*).
21. Although ages on the rims of the crystal vary from 440 to 420 Ma (Fig. 1), they are systematic with respect to distance from the presumed center of the crystal (Fig. 2B). We interpret that the distance from point c in Fig. 1 to the perimeter of the original crystal was a roughly uniform 1000 μm, and ages of about 430 to 440 Ma presently occur along edges broken during sample preparation.

22. We thank A. Albee for providing the samples for this study. This manuscript was improved by thoughtful reviews from G. B. Dalrymple and T. C. Onstott and discussions with R. J. Cumbest and W. J. Olszweski.

16 April 1993; accepted 26 July 1993

Activation of Floral Homeotic Genes in *Arabidopsis*

Detlef Weigel* and Elliot M. Meyerowitz†

The identity of floral organs in *Arabidopsis thaliana* is determined by homeotic genes, which are expressed in specific regions of the developing flower. The initial activation of homeotic genes is accomplished at least in part by the products of two earlier acting genes with overlapping functions. These are the floral meristem–identity genes *LEAFY* and *APETALA1*. The requirements of *LEAFY* and *APETALA1* activity vary for different homeotic genes.

Flowers of *Arabidopsis* are composed of four types of organs: sepals, petals, stamens, and carpels. The floral organs are arranged in concentric rings, or whorls. Sepals occupy the first, outermost whorl, petals the second whorl, stamens the third whorl, and carpels, which form the central gynoecium, the fourth, central whorl. Organ identity in the flower is determined by three classes of homeotic genes, A, B, and C, each of which acts in two adjacent whorls. In this way, every whorl has a distinct combination of homeotic functions: class A alone in the first whorl, classes A and B in the second whorl, classes B and C in the third whorl, and class C alone in the fourth whorl (*1*). In all cases in which the RNA expression pattern has been reported, RNA of a homeotic gene accumulates in those whorls of the wild-type flower where the gene is active, as deduced from its mutant phenotype (*2–6*).

The region-specific expression of homeotic genes is brought about mainly by negative interactions. For example, the expression of the class C gene *AGAMOUS* (*AG*) is repressed in the outer whorls by the class A gene *APETALA2* (*AP2*) (*1, 3*), and the expression of the class B genes *APETALA3* (*AP3*) and *PISTILLATA* (*PI*) is repressed in the central whorl by the whorl-identity gene *SUPERMAN* (*6–8*). However, little is known about the initial activation of homeotic genes, probably accomplished by positive regulators. The candidates for such activators are two genes, *LEAFY* (*LFY*) and *APETALA1* (*AP1*), that control floral meristem identity and whose inactivation causes the partial transformation of flowers into shoots (*9–13*). The determination of floral meristem identity precedes that of floral organ identity, and consistent with this early function, the expression of *LFY* and *AP1* is initiated earlier than that of the homeotic genes (*5, 11*). To understand better the effect of *LFY* and *AP1* on homeotic gene activity, we analyzed how *lfy* and *ap1* mutations affect the expression of homeotic genes that determine floral organ identity.

The two B function genes *AP3* and *PI* are expressed in the developing second and third whorls, which give rise to petals and stamens (*4, 6*) (Figs. 1A and 2A). Second- and third-whorl organs are affected differently by *ap1-1* and *lfy-6* mutations, both of which are apparently complete loss-of-function alleles (*14*). In *ap1-1* mutants, the stamens of the third whorl are normal, but second-whorl organs typically fail to develop (*9, 13*). In *lfy-6* mutant flowers, none of the inner

California Institute of Technology, Division of Biology 156-29, Pasadena, CA 91125.

*Present address: Department of Biology 0116, University of California, San Diego, La Jolla, CA 92093.
†To whom correspondence should be addressed.

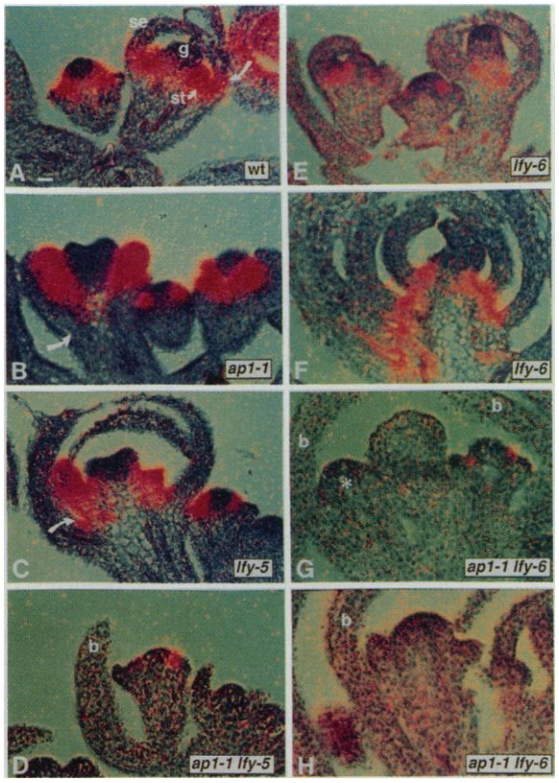

Fig. 1. Expression of *AP3* RNA in wild-type and mutant flowers detected by in situ hybridization. (**A**) In young wild-type flowers, *AP3* RNA is detected in developing petals and stamens (st), but is largely absent from sepals (se) and the gynoecium (g), which is composed of the two central carpels. Petals are still small and not visible in most sections. Expression at the base of the sepal in the stage 7 flower to the right is indicated by the arrow; scale bar, 20 μm. (**B**) In *ap1-1* flowers, *AP3* is expressed as it is in wild type. No *AP3* RNA is present in the base of first-whorl organs (arrow). (**C**) In *lfy-5* flowers, the *AP3* pattern is largely normal, although the domains are sometimes reduced as in the stage 4 flower to the right. Expression at the adaxial base of the first-whorl sepals appears in the older flower to the left (arrow). (**D**) In most *ap1-1 lfy-5* flowers, no *AP3* RNA is detected. This panel shows an unusual stage 3 flower in which some *AP3* RNA is detected. The expression is not in a symmetric pattern. The transformed flower is subtended by a bract (b). (**E**) In young *lfy-6* flowers, both the amount and domains of *AP3* RNA are reduced. (**F**) In this older *lfy-6* flower, *AP3* RNA is present at the base of most organs, concentrated more at their adaxial sides. (**G**) In most *ap1-1 lfy-6* flowers, no *AP3* RNA is detected, as in the stage 3 flower to the left (asterisk). Rarely, small amounts of *AP3* RNA are present, as in the stage 3 flower to the right. (**H**) Another typical *ap1-1 lfy-6* flower without any detectable *AP3* RNA. The stages are from (*26*) and the relative magnifications are ×1.28 in (D), (G), and (H) and ×1.0 in the other panels.

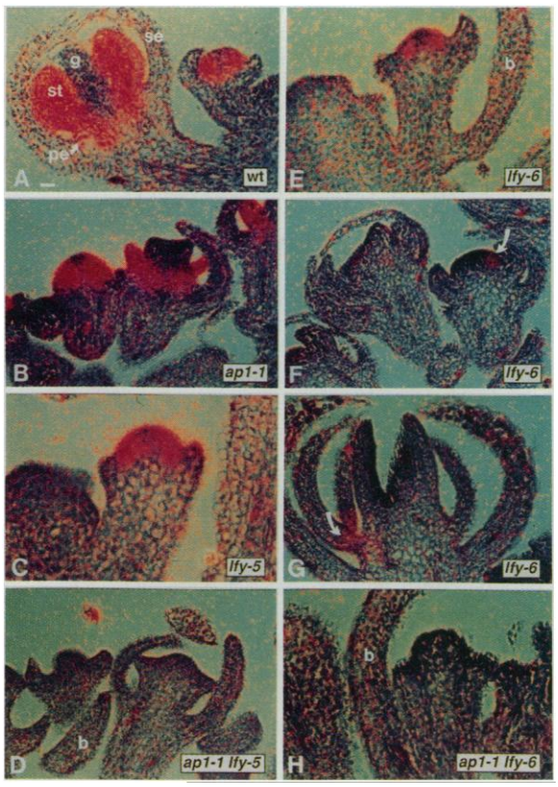

Fig. 2. Expression of *PI* RNA in wild-type and mutant flowers detected by in situ hybridization. (**A**) In wild type, *PI* is expressed in petals (pe) and stamens but not in sepals or the central gynoecium. Abbreviations as in Fig. 1; scale bar, 20 μm. A similar pattern is observed in (**B**) *ap1-1* and (**C**) *lfy-5* flowers. (**D**) In these *ap1-1 lfy-5* flowers, no *PI* RNA is detected. (**E** and **F**) The amount and domains of *PI* RNA are reduced in *lfy-6* flowers to various degrees. Asymmetric *PI* expression (arrow) appears in the flower to the right in (F). (**G**) In this exceptional older *lfy-6* flower, some *PI* RNA is detected at the base of two organs (arrow). (**H**) A typical *ap1-1 lfy-6* flower, in which no *PI* RNA is detected. Bracts are indicated in (D), (E), and (H). The relative magnifications are ×1.6 in (C), ×1.28 in (E) and (H), and ×1.0 in the other panels.

three whorls can be clearly distinguished. Almost all organs are either leaf-, sepal-, or carpel-like, and only rarely do mosaic organs with partial petal or stamen character develop (*11*, *15*). The distinct phenotypes of mature *ap1-1* and *lfy*-6 flowers correlate with differences in the effects of *lfy*-6 and *ap1-1* mutations on *AP3* and *PI* expression patterns, as determined by in situ hybridization (*16*). The amount of *AP3* and *PI* RNA and the timing of expression appear normal in young *ap1-1* flowers (Figs. 1B and 2B), although the expression domains often seem somewhat smaller than those in wild type. This difference might be related to the absence of the (initially small) second-whorl organ primordia in most *ap1-1* flowers. In contrast, both the amounts of *AP3* and *PI* RNA and the domains of expression are severely reduced in young *lfy*-6 flowers (Figs. 1E and 2, E and F). Because *AP3* and *PI* expression patterns are similar in wild type, it is surprising that in *lfy*-6 flowers the amount of *PI* RNA is more reduced than the amount of *AP3* RNA, especially at later stages (compare Fig. 1F with Fig. 2G) (*17*). The observed reduction of *AP3* and *PI* RNA in young *lfy*-6 flowers corroborates the assertion that *LFY* exerts its role in determining floral meristem identity at an early stage, that is, before floral organs differentiate. This reduction also supports the argument that insufficient activation of the homeotic B function is responsible for the absence of petals and stamens in severe *lfy* alleles (*11*, *12*).

The removal of *AP1* activity greatly enhances the transformation of flowers into shoots in *lfy* mutants (*11*–*13*). Therefore, we wondered whether the residual expression of *AP3* and *PI* in *lfy*-6 might be due to *AP1* activity. When we analyzed *ap1-1 lfy*-6 double mutants, we did not detect *AP3* or *PI* RNAs in most flowers (Figs. 1, G and H, and 2H). In the few flowers where some expression is evident, the amount of RNA is much lower than in *lfy*-6 single mutants (compare Fig. 1G with Fig. 1E). This result indicates that *AP1* is required for the activation of *AP3* and *PI* but that this function of *AP1* is largely masked in the presence of *LFY* activity. The overlapping action of *LFY* and *AP1* is even more dramatically revealed by a weak loss-of-function allele such as *lfy*-5, in which *LFY* activity is merely reduced rather than completely eliminated. Petals and stamens, which are specified by the homeotic B function, develop in *lfy*-5 flowers, although they are often abnormal, and their numbers are reduced (*11*). As in *ap1-1* flowers, *AP3* and *PI* expression are much more normal in *lfy*-5 flowers than in flowers from plants homozygous for the strong *lfy*-6 allele (Figs. 1C and 2C). In contrast, *AP3* and *PI* RNAs

are rarely detected in *ap1-1 lfy-5* double mutant flowers (compare Figs. 1, B and C, with Fig. 1D and Fig. 2, B and C, with Fig. 2D). Taken together, these results show that *LFY* and *AP1* are positive regulators of *AP3* and *PI* expression.

The C class of homeotic genes is represented by AG, which is expressed in the center of developing wild-type flowers. The expression domain of AG demarcates the presumptive third and fourth whorls, in which stamens and carpels develop (*2, 3*) (Fig. 3A). In addition to controlling stamen and carpel identity, AG regulates floral meristem determinacy, such that *ag* mutants develop new flowers in place of the fourth whorl (*1, 18*) (Fig. 4A). The third and fourth whorls are largely normal in *ap1-1* flowers but cannot be identified unambiguously in *lfy*-6 because the organs interior to the first whorl often develop in an abnormal pattern (*11*). Organs with carpel character, however, are present in *lfy*-6 flowers. Double mutant phenotypes indicate that AG is active in *lfy*-6 and *ap1-1* mutants, because *ap1 ag* and *lfy ag* double mutants have phenotypes distinct from those of *ap1* or *lfy* single mutants (*9, 11–13*) (Fig. 4, B and C).

The distribution of AG RNA appears normal in most *ap1-1* flowers (Fig. 3B) (*19*). Although AG RNA accumulates in the center of older *lfy*-6 flowers (Fig. 3C), which is similar to what is observed in wild-type flowers, the early pattern of AG expression in *lfy*-6 is abnormal. The onset of AG expression is delayed, and when AG RNA is first detected it is confined to a smaller domain than in wild type (compare Fig. 3C with Fig. 3A). Because the later expression pattern of AG in *lfy*-6 appears more normal than the early pattern, we assume that, contrary to the case in wild type, the AG RNA domain expands in *lfy*-6 mutant flowers (*20*). In addition to the changes in AG expression in the flower, the *lfy*-6 mutation has an unexpected effect on the floral specificity of AG expression: AG RNA becomes ectopically expressed in the stem of *lfy*-6 mutants as well as in some of the bracts that subtend *lfy*-6 flowers (Fig. 3D). The ectopic expression does not appear to have any functional relevance, because neither the carpellody of bracts nor the morphology of inflorescence stems is altered in *lfy*-6 *ag-2* double mutants compared with *lfy*-6 single mutants (*11, 21*).

In contrast to either *lfy*-6 or *ap1-1* single mutants, *ap1-1 lfy*-6 double mutants have a pattern of AG expression that does not bear any resemblance to the pattern in wild type. Whereas AG RNA is detected in the center of wild-type *ap1-1* and *lfy*-6 flowers, it does not accumulate in the center of *ap1-1 lfy*-6 double mutant flowers (compare Fig. 3E with Figs. 3, A to C). However, AG RNA is detected in the stem of *ap1-1 lfy*-6 double mutants, in bracts subtending the flowers, and in what appear to be ectopic sites in the flowers (Figs. 3, E and F). The ectopic expression pattern in *ap1-1 lfy*-6 is similar to that observed in *lfy*-6 single mutants. We believe that the abnormal expression pattern in the flowers, which are transformed into shoot-like structures, is equivalent to the ectopic expression in the stem and bracts of the main shoot. Because the normal function of AG is in the center of the flower, where it regulates stamen and carpel identity and controls floral meristem determinacy, we suspected that the apparently ectopic expression of AG in *ap1-1*

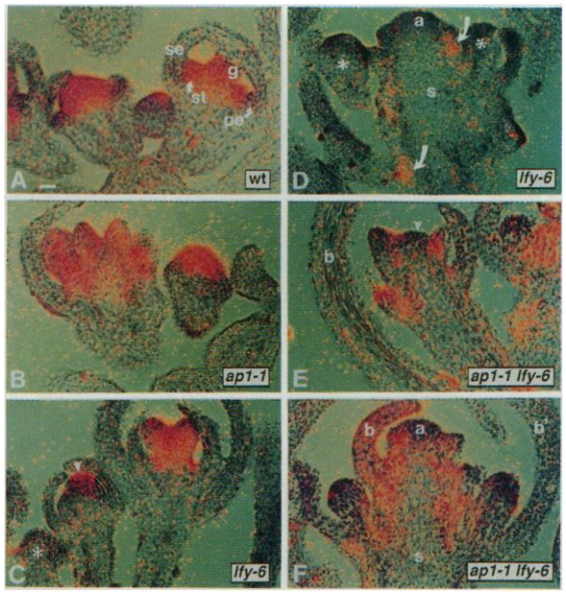

Fig. 3. Expression of *AG* RNA in wild-type and mutant plants detected by in situ hybridization. (**A**) In young wild-type flowers, *AG* is expressed in stamens and in the gynoecium but not in sepals or petals. The stage 3 flower in the center is sectioned tangentially; consequently, this section does not show the full extent of the *AG* domain. Abbreviations as in Fig. 1. (**B**) The *AG* pattern is normal in most *ap1-1* flowers. (**C**) In a young *lfy-6* flower (asterisk), which is roughly equivalent in age to the wild-type flower in the center of (A), no *AG* RNA is detected. In the flower in the center, equivalent to stage 5 of wild type, a small central domain of *AG* expression is apparent (arrowhead). In older *lfy-6* flowers, as in the one to the right, *AG* is expressed in several organ primordia in the center. (**D**) This longitudinal section, which includes the apex (a), shows ectopic expression (arrows) in the stem (s) of an *lfy-6* inflorescence. Asterisks indicate two young flower primordia. (**E**) In this *ap1-1 lfy-6* flower, *AG* RNA is detected at several sites but not in the center of the flower, where it is normally found (arrowhead). The flower is subtended by a bract. (**F**) Ectopic expression of *AG* RNA is prominent in the stem of an *ap1-1 lfy-6* inflorescence. A signal is detected in the bract to the left but not in the one to the right (b′), demonstrating the irregularity of ectopic *AG* expression. The bar in (A) represents 20 μm in all panels.

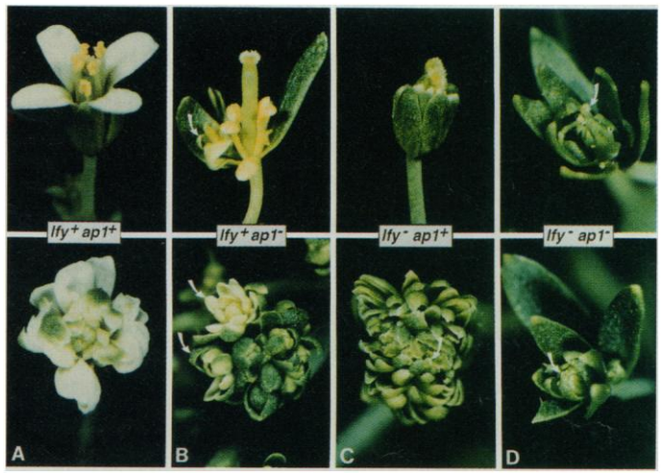

Fig. 4. Effect of the strong *ag-2* mutation in the presence or absence of *LFY* and *AP1* activity. The top panels show mature flowers that carry a wild-type allele at the *AG* locus, whereas the bottom panels show *ag-2* homozygous flowers. (**A**) Expression of the *ag* mutant phenotype in lfy^+ $ap1^+$. Stamens and carpels are absent in the *ag-2* single mutant flower, which is indeterminate. In the presence of an *LFY* wild-type allele, none of the organs in an *ag-2* flower have carpelloid character. (**B**) Expression of the *ag* mutant phenotype in lfy^+ *ap1-1* ($ap1^-$). Arrows indicate secondary flowers, which are particularly abundant in the *ap1-1 ag-2* double mutant. The petals are partially restored in the double mutant. (**C**) Expression of the *ag* mutant phenotype in *lfy-6* (lfy^-) $ap1^+$. Stigmatic tissue (arrow), indicative of carpelloid character, appears in *lfy-6 ag-2* double mutants. (**D**) Expression of the *ag* mutant phenotype in *lfy-6 ap1-1* (lfy^- $ap1^-$). *The* ag^+ and ag^- genotypes look similar. Arrows indicate stigmatic tissue. The *lfy-6 ap1-1 ag-2* triple mutants were identified by polymerase chain reaction as described (*11*).

lfy-6 flowers is functionally irrelevant. We tested this hypothesis by generating *lfy-6 ap1-1 ag-2* triple mutants; their phenotype is indistinguishable from the phenotype of *ap1-1 lfy-6* double mutants, confirming that AG does not have any overt function in the absence of *LFY* and *AP1* activity (Fig. 4D).

The results here demonstrate that expression of the homeotic genes *AP3*, *PI*, and AG requires the activity of the meristem-identity genes *LFY* and *AP1*. Furthermore, we have shown that homeotic genes differ in their requirements for *LFY* and *AP1* activity. None of the homeotic genes studied are affected strongly by the loss of *AP1* activity alone. The effects of *AP1* and *LFY* on AG overlap, and only the elimination of both *AP1* and *LFY* activities completely abolishes the normal pattern of AG expression. In contrast, *LFY* is a major activator of *AP3* and *PI*, as indicated by the severe reduction of their RNA amounts in strong *lfy-6* single mutants. The function of *AP1* in activating *AP3* and *PI* only becomes obvious when *LFY* activity is reduced or eliminated.

Even in *ap1-1 lfy-6* double mutants, some remnants of the normal patterns of homeotic gene expression were observed. Because the available evidence suggests that both *lfy-6* and *ap1-1* represent complete loss-of-function alleles (*14*), other factors likely act in concert with *LFY* and *AP1* to activate homeotic gene expression. Clearly, *LFY* and *AP1* have overlapping functions in the activation of homeotic gene expression. The molecular interactions that result in the coordinate action of *LFY*, which encodes a nuclear protein that is not a member of any known family of transcription factors (*11, 22*), and *AP1*, which encodes a protein with similarity to MADS-box transcription factors (*5*), have yet to be determined. Further experiments are also required to determine whether the observed interactions between *LFY* and *AP1* and the homeotic genes are direct.

We do not know why different *Arabidopsis* homeotic genes vary in their requirements for the activity of upstream regulators. However, if the same scenario holds for other species of flowering plants, it is likely that adjustments in the activity of upstream regulators could have complex effects on the expression of downstream homeotic genes, and thus on the overall pattern of organs in the flower. Homologs for many of the genes analyzed in this study have been found in other species (*23, 24*), and similar studies in other species might help determine how regulatory interactions between floral meristem–identity and homeotic genes have changed during the evolution of flowering plants. That mutations in the cognate homologs of *LFY* and *AP1* in the distantly related species *Antirrhinum* (*23*) cause phenotypes quite different from mutations in their *Arabidopsis* counterparts already indicates that such changes have occurred.

REFERENCES AND NOTES

1. J. L. Bowman, D. R. Smyth, E. M. Meyerowitz, *Development* **112**, 1 (1991).
2. M. F. Yanofsky *et al.*, *Nature* **346**, 35 (1990).
3. G. N. Drews, J. L. Bowman, E. M. Meyerowitz, *Cell* **65**, 991 (1991).
4. T. Jack, L. L. Brockman, E. M. Meyerowitz, *ibid.* **68**, 683 (1992).
5. M. A. Mandel, C. Gustafson-Brown, B. Savidge, M. F. Yanofsky, *Nature* **360**, 273 (1992).
6. K. Goto and E. M. Meyerowitz, unpublished results.
7. E. A. Schultz, F. B. Pickett, G. W. Haughn, *Plant Cell* **3**, 1221 (1991).
8. J. L. Bowman *et al.*, *Development* **114**, 599 (1992).
9. V. F. Irish and I. M. Sussex, *Plant Cell* **2**, 741 (1990).
10. E. A. Schultz and G. W. Haughn, *ibid.* **3**, 771 (1991).
11. D. Weigel, J. Alvarez, D. R. Smyth, M. F. Yanofsky, E. M. Meyerowitz, *Cell* **69**, 843 (1992).
12. E. Huala and I. M. Sussex, *Plant Cell* **4**, 901 (1992).
13. J. L. Bowman, J. Alvarez, D. Weigel, E. M. Meyerowitz, D. R. Smyth, *Development*, in press.
14. In *lfy-6*, a premature stop codon truncates the open reading frame after less than a tenth of its length (*11*) and no protein is detected (*22*), indicating that *LFY* activity is completely eliminated. The sequence change in the *ap1-1* allele does not allow for a similar conclusion (*5*). However, its phenotype is virtually identical to another *ap1* allele that carries a mutation predicted to inactivate the DNA binding domain of the *AP1* protein (A. Mandel and M. Yanofsky, personal communication), suggesting that *ap1-1* also represents the complete loss-of-function state.
15. The early-arising flowers in *lfy* mutants are completely transformed into shoots, whereas the late-arising flowers are only partially transformed (*10–12*). For the experiments reported here, only the late-arising flowers were analyzed.
16. In situ hybridizations were performed with *AP3* (*4*), *PI* (*6*), and *AG* (*2, 3*) probes as described (*3*). To ensure comparability of in situ hybridization to wild-type and mutant tissues, sections of mutant and wild-type flowers were processed in the same experiments and, in several instances, on the same slide. All experiments were done with complete serial sections. Changes in the spatial domains of expression and in the amount of signal were only recorded when they could be confirmed in adjacent sections and when they were consistent for the majority of flowers analyzed. Changes in signal intensity (the concentration of silver grains) described here were all severalfold, with the signal completely absent in many cases. Exposure times were from 3 to 6 weeks to reveal weak signals in mutants. All photographs were taken on Fuji (Tokyo) Velvia professional film as double exposures with bright-field illumination to visualize the tissue and dark-field illumination to visualize silver grains. For the dark-field view, a red filter was used.
17. Unlike *PI* RNA, *AP3* RNA is detected in older *lfy-6* flowers at the base of many organs, most of which have sepal character (Figs. 1F and 2G). When we analyzed wild-type flowers more carefully, we found that *AP3* RNA but not *PI* RNA is sometimes detectable at the base of first-whorl sepals (Figs. 1A and 2A). However, the amount of *AP3* RNA in wild-type sepals was usually much lower than in the sepaloid organs of *lfy-6* mutants, including the outermost organs. Thus, the significance of the late expression pattern of *AP3* in *lfy-6* remains unclear. No *AP3* RNA was detected in the first-whorl organs of *ap1-1* mutants (Fig. 1B).
18. J. L. Bowman, D. R. Smyth, E. M. Meyerowitz, *Plant Cell* **1**, 37 (1989).
19. In a few *ap1-1* flowers, particularly in secondary flowers forming in the axils of first-whorl organs, *AG* is ectopically expressed in the outer whorls. This expression is consistent with the observation that first-whorl organs are occasionally carpelloid (and more frequently so in the secondary flowers) and that second-whorl organs are sometimes transformed into stamens (*13*), thus corroborating the assertion that *AP1* has a dual role in controlling floral meristem identity and in executing the homeotic A function (*5, 13*). Because of the small size of the petal anlagen in stage 3 flowers and the failure of these organs to develop in most flowers, we cannot exclude the possibility that *AG* expression occasionally expands only into the second whorl and not into the first whorl. Axillary flowers of *ap1-1 ag-2* double mutants develop petals more frequently than *ap1-1* single mutant flowers (Fig. 4B) (*13*), which suggests that *AG* has some role in suppressing petal development in *ap1-1* mutants.
20. An obvious expansion of the *AG* RNA domain is not observed in developing wild-type flowers (*3*) but could take place, although much faster than in *lfy-6* mutants. Alternatively, this difference in the temporal pattern of *AG* expression might reflect the aberrant nature of the *lfy-6* floral meristem, which is partially transformed into a shoot meristem. The central cells in an *lfy-6* floral meristem might proliferate more than the corresponding cells in a wild-type floral meristem, and an initial defect in the spatial pattern of *AG* expression could be compensated later by an increased proliferation of cells that express *AG*.
21. Because *AG* is known to be expressed in carpels at later stages of flower development (*25*), expression of *AG* in bracts of *lfy* mutants is likely a consequence rather than a cause of the often carpelloid nature of bracts, which are not found in wild type. The expression in *lfy-6* stems, which is mostly confined to the outer cell layers, was followed through adjacent serial sections and was absent from wild-type stems. We do not have any explanation for this observation. Because *LFY* is not expressed in the stems of wild-type plants, the observed derepression of *AG* indicates a nonautonomous effect of the *lfy* mutation.
22. D. Weigel, L. Goh, E. M. Meyerowitz, unpublished results.
23. E. S. Coen *et al.*, *Cell* **63**, 1311 (1990); P. Huijser *et al.*, *EMBO J.* **11**, 1239 (1992).
24. H. Sommer *et al.*, *EMBO J.* **9**, 605 (1990); L. Pnueli, M. Abu-Abeid, W. Nacken, Z. Schwarz-Sommer, E. Lifschitz, *Plant J.* **1**, 255 (1991); Z. Schwarz-Sommer *et al.*, *EMBO J.* **11**, 251 (1992); G. C. Angenent, M. Busscher, J. Franken, J. N. M. Mol, A. J. van Tunen, *Plant Cell* **4**, 983 (1992); D. Bradley, R. Carpenter, H. Sommer, N. Hartley, E. Coen, *Cell* **72**, 85 (1993); W. Tröbner *et al.*, *EMBO J.* **11**, 4693 (1992); D. Weigel and E. M. Meyerowitz, in *Molecular Basis of Morphogenesis*, M. Bernfield, Ed. (Wiley, New York, 1993), pp. 91–105.
25. J. L. Bowman, G. N. Drews, E. M. Meyerowitz, *Plant Cell* **3**, 749 (1991).
26. D. R. Smyth, J. L. Bowman, E. M. Meyerowitz, *ibid.* **2**, 755 (1990).

27. We thank members of the Meyerowitz lab and S. Alvarez, H. Baribault, J. Bowman, A. Golden, A. Mandel, D. Smyth, P. Sternberg, and M. Yanofsky for critical review of the manuscript; T. Jack for discussing the *AP3* expression pattern; T. Jack, A. Mandel, M. Yanofsky, and especially K. Goto for providing probes before publication; and A. Mandel and M. Yanofsky for communicating unpublished results. Supported by the American Cancer Society, California Division, through a Senior Postdoctoral Fellowship (D.W.), the Human Frontier Science Program; and U.S. Department of Energy Division of Energy Biosciences grant DE-FG03-88ER13873 (E.M.M.).

5 May 1993; accepted 2 July 1993